J. Membrane Biol. 175, 35–52 (2000)

The Journal of
Membrane
Biology

Direct Comparison of NPPB and DPC as Probes of CFTR Expressed in *Xenopus* Oocytes

Z.-R. Zhang, S. Zeltwanger, N.A. McCarty

Departments of Physiology and Pediatrics, Center for Cell and Molecular Signaling, Emory University School of Medicine, Atlanta, GA 30322, USA

Received: 14 October 1999/Revised: 18 January 2000

Abstract. Blockers of CFTR with well-characterized kinetics and mechanism of action will be useful as probes of pore structure. We have studied the mechanism of block of CFTR by the arylaminobenzoates NPPB and DPC. Block of macroscopic currents by NPPB and DPC exhibited similar voltage-dependence, suggestive of an overlapping binding region. Kinetic analysis of single-channel currents in the presence of NPPB indicate drug-induced closed time constants averaging 2.2 msec at −100 mV. The affinity for NPPB calculated from single-channel block, K_D = 35 μM, exceeds that for other arylaminobenzoates studied thus far. These drugs do not affect the rate of activation of wild-type (WT) channels expressed in oocytes, consistent with a simple mechanism of block by pore occlusion, and appear to have a single binding site in the pore. Block by NPPB and DPC were affected by pore-domain mutations in different ways. In contrast to its effects on block by DPC, mutation T1134F-CFTR decreased the affinity and reduced the voltage-dependence for block by NPPB. We also show that the alteration of macroscopic block by NPPB and DPC upon changes in bath pH is due to both direct effects (i.e., alteration of voltage-dependence) and indirect effects (alteration of cytoplasmic drug loading). These results indicate that both NPPB and DPC block CFTR by entering the pore from the cytoplasmic side and that the structural requirements for binding are not the same, although the binding regions within the pore are similar. The two drugs may be useful as probes for overlapping regions in the pore.

Key words: Cystic fibrosis — Cystic fibrosis transmembrane conductance regulator — Chloride channel blocker — Anion channel — Arylaminobenzoate

Correspondence to: N.A. McCarty

Introduction

Cystic fibrosis (CF) is the result of mutations in a single gene [39], that which encodes a large membrane protein called the Cystic Fibrosis Transmembrane conductance Regulator (CFTR). The CFTR protein forms an epithelial Cl^- channel which is activated by protein kinase A (PKA) phosphorylation plus ATP hydrolysis [15], and is expressed predominantly in epithelial cells. The CFTR molecule is constructed in modular fashion from two nonidentical halves, each consisting of six transmembrane-spanning (TM) domains followed by a nucleotide-binding domain; the two halves are connected by a regulatory (R) domain [39].

A great deal of effort has been spent in attempts to define what portions of this protein line the permeation pathway; recent reviews on this topic have been published [8, 41, 46]. One approach to structure-function studies of the permeation pathway in ion channels relies upon having molecular probes, in the form of blocking drugs, which have a reasonably clear mechanism of action. For rapid screening of pore-domain mutations, it is helpful if the drugs can be used in whole-cell experiments; interesting mutants would then be subjected to more detailed kinetic analysis by single-channel recording. While several classes of compounds have been proposed as blockers of CFTR, few have been shown to fit these criteria (clarity of mechanism, ease of use) in order to be considered as useful probes for structure-function experiments [41]. CFTR channels are characterized by: their sensitivity to block by intracellular [26] but not extracellular disulfonic stilbenes, such as DIDS and SITS; their blockade by the sulfonylurea hypoglycemic agent glibenclamide [40, 44, 45, 53] and its congener tolbutamide [55]; and their blockade by arylaminobenzoates such as diphenylamine-2-carboxylate (DPC), flufenamic acid (FFA), and 5-nitro-2- (3-phenylpropylamino)-benzoate (NPPB). We have investigated previ-

ously the utility of DPC and FFA as molecular probes for the channel pore. These compounds block CFTR from the cytoplasmic side in a voltage-dependent manner [33] while their block of the outward rectifier of epithelial cells and of the background channel in *Xenopus* oocytes is only weakly voltage-dependent and occurs from the extracellular side [52, 61, 64]. Block of the cardiac and epithelial forms of CFTR by NPPB has also been investigated [56, 58].

Bath application of DPC to oocytes expressing WT CFTR led to voltage-dependent block of cAMP-activated currents [33]. Woodhull analysis [63] indicated that the DPC binding site lies approximately 40% of the distance through the electrical field, as measured from the cytoplasmic side. FFA, which differs from DPC by the addition of a trifluoromethyl group to the phenyl ring, blocked whole-cell currents similarly, although with somewhat greater efficacy due to a slower off-rate. DPC and FFA are permeant blockers of CFTR, able to reach their binding site(s) when applied from either side of a membrane patch. This is likely due to extracellular drug accessing the cytoplasmic side via the membrane phase [33, 35, 58]. Block by DPC and FFA leads to disruptions of single channel current of resolvable duration as a result of quantifiable interactions between drug and channel [33]. The characteristics of block and the finding that DPC interacts with Cl^- during permeation [35] indicated that DPC blocks by an open-channel mechanism. NPPB is a congener of the parent molecule, DPC; this drug has a lengthened aliphatic chain between the benzoate and phenyl rings, and an electron-withdrawing nitryl group on the benzoate ring. It is assumed that NPPB blocks CFTR by a mechanism similar to that of DPC. Previous data from other laboratories [56, 58] suggested that NPPB blocked cardiac CFTR with a voltage dependence less steep than that of DPC block of epithelial CFTR expressed heterologously in oocytes. One goal of the present study, therefore, was to compare these drugs under identical conditions.

We have shown previously that residues in TM domain number six (TM6) and in TM12 contribute to the binding sites for DPC [35]. However, the binding sites for NPPB and glibenclamide have not been determined, although initial findings suggest that NPPB binding is sensitive to charge at the extracellular end of the pore [56]. Furthermore, the mechanism of block by these drugs is not certain. Indeed, although block of CFTR by NPPB was first described in 1992 [7], the mechanism of action at the single channel level has not been characterized. In this report, we compare NPPB and DPC as probes for structure-function experiments of CFTR expressed in *Xenopus* oocytes. Our goals were: (i) to determine whether NPPB may serve as a useful probe of the pore, indicated by clarity of mechanism both for macroscopic and single-channel blockade; (ii) to determine whether the interaction between these drugs and the pore is pH-dependent; and (iii) to determine if the drugs might serve as probes for different regions of the pore, by virtue of differential sensitivity to mutations in pore-lining domains. We show that NPPB and DPC function as simple pore-blockers, and that they differ in their efficacy, pH-dependence, and sensitivity to mutations within the pore of CFTR. Differences in the blocking behavior of these drugs suggest that they will serve as probes for different regions of the pore. Portions of these data have been published previously in abstract form [68].

Materials and Methods

Preparation of Oocytes and cRNA Injection

The methods used are similar to those described previously [33, 35]. Briefly, stage V-VI oocytes from female *Xenopus* were prepared as described [37] and were incubated at 18°C in a modified Liebovitz's L-15 medium with addition of HEPES (pH 7.5), gentamicin, and penicillin/streptomycin. cRNA was prepared from a construct carrying the full coding region of CFTR in the pAlter vector (Promega; Madison, WI). Oocytes were injected with 5 to 19 ng of CFTR cRNA plus 0.6 ng of cRNA for the human β-2 adrenergic receptor (β_2-AR), which allows activation of PKA-regulated currents by addition of isoproterenol (ISO) to the bath. Recordings were made at room temperature, 42–96 hr after injection. Construction of S341A-CFTR and T1134F-CFTR was described previously [35].

Electrophysiology

Standard two-electrode voltage clamp techniques were used to study whole-cell currents. Electrodes were pulled in four stages from borosilicate glass (Sutter Instrument, Novato, CA) and filled with 3 M KCl. Pipette resistances measured 0.4–0.9 MΩ in bath solution. Two-electrode voltage clamp data were acquired at room temperature (~22°C) using a GeneClamp 500 amplifier and pCLAMP software (Axon Instruments, Foster City, CA); macroscopic currents were filtered at 500 Hz. Normal bath solution for whole-cell experiments (ND96) was nominally Ca-free and contained (in mM): 96 NaCl, 2 KCl, 1 $MgCl_2$, and 5 HEPES [33]. For different experiments, the pH of the bath solution was adjusted to 6.5, 7.5, or 8.0 with NaOH. Oocytes were activated by superfusion of ND96 containing ISO at 0.1–5 μM final concentration. For experiments including NPPB, all solutions contained 1 mM Ba^{2+} to limit activation of endogenous Cl^- channels.

Single CFTR channels were studied in excised, inside-out patches at room temperature. Oocytes were prepared for study by shrinking in hypertonic solution (in mM: 200 monopotassium aspartate, 20 KCl, 1 $MgCl_2$, 10 EGTA, and 10 HEPES-KOH, pH 7.2) followed by manual removal of the vitelline membrane. Pipettes were pulled in 4 stages from borosilicate glass (Sutter), and had resistances averaging ~10 MΩ when filled with pipette solution (in mM: 150 NMDG-Cl, 5 $MgCl_2$, and 10 TES, adjusted to pH 7.4 with Tris). Typical seal resistances were in the range of 200 GΩ. Channels were either activated on-cell with ISO before excising into intracellular solution (150 NMDG-Cl, 1.1 $MgCl_2$, 2 Tris-EGTA, 1 MgATP, 10 TES, pH 7.3, and 50U/mL PKA (Promega), or were activated by PKA following excision. Patch currents were measured with an AI2120 amplifier (Axon), and were recorded at 10 kHz on DAT tape (Sony, model DTC-790). For subsequent analysis, records were filtered at 1 kHz (4-pole Bessel filter, Warner Instru-

ments; Hamden, CT) and acquired by the computer at 100 μsec/point using the Fetchex program of pCLAMP (Axon).

Analysis of Macroscopic Steady-State Block

For construction of steady-state current-voltage (*I-V*) relations and calculation of voltage dependence of block, the membrane potential was stepped for 75 msec from the holding potential (−30 mV) to a range of potentials from −140 to +80 mV, at 20 mV increments. Currents were analyzed using the Clampfit program, version 6.04 (Axon). The current at each potential before exposure to ISO and after washout was subtracted to determine the cAMP-dependent current. Data were taken from the final 30 msec of the 75 msec step to each potential and averaged. Apparent K_D was calculated as

$$Apparent\ K_D^{(V)} = [\text{drug}]_{bath} \cdot \frac{I}{I_o - I} \quad (1)$$

where for each voltage *V*, I_o is the current level in the absence of blocker and *I* is the current level after several minutes of treatment with drug. In this context, it is important to point out that we do not know the actual concentration of drugs in the cytoplasm during whole-cell experiments; we have estimated this, as discussed below. Voltage dependence of block was calculated as

$$K_D^{(V)} = K_D^{(0)} \cdot \exp(z\theta FV/RT) \quad (2)$$

where $K_D^{(0)}$ is the K_D at 0 mV, *z* is the valence (assumed to be −1 for both NPPB and DPC [33, 58]), θ is the electrical distance sensed by the blocker at its binding site, calculated from the cytoplasmic end of the pore, and *F, V, R,* and *T* have their usual meanings. For these experiments, we assumed that there is a single binding site for NPPB and DPC; we have tested this notion, as shown below.

Nonstationary Analysis of Blockade

Some of the experiments in this study required a means of quantitating macroscopic channel block as rapidly as possible. Because both the on-rates and off-rates for the interaction of arylaminobenzoates with CFTR are fast [33], it is impossible to accurately measure time-constants of block from whole-cell experiments (*see also* [57]). Voltage-jump experiments do not allow estimation of on-rates and off-rates in the traditional way by calculation of time-constants for block and relief from block. This is evidenced by the rapid block of CFTR currents seen following a step to a hyperpolarizing potential, at which the affinity for blockade by NPPB or DPC is high (*see* Fig. 1), and the rapid unblock seen at depolarizing potentials, at which the affinity is low. Indeed, this time-independence of macroscopic block has led some investigators to propose that arylaminobenzoates inhibit CFTR by an allosteric mechanism rather than by pore blockade. A series of steps to a range of voltages requires seconds to perform. Hence, we developed a protocol (which we call "nonstationary analysis") to allow quantitation of voltage dependent block more rapidly than is possible using voltage steps (*see* Fig. 7). The time-independent character of blockade by DPC and NPPB allows estimation of blockade using a voltage ramp. Oocytes were activated by ISO for 6–7 min in the presence or absence of drugs. From a holding potential of −30 mV, the membrane potential was stepped to +40 mV for 465 msec (which drives the drug off of its binding site), stepped to −20 mV for 5 msec and then ramped to −100 mV over 50 msec. The magnitude and duration of each of the potential steps and of the ramp were optimized to avoid capacitance artifacts and to limit activation of endogenous oocyte channels.

Current traces in the absence of blocker exhibit some curvature due to Goldman rectification and due to blockade by large cytoplasmic molecules [23]; the curvature is increased in the presence of blockers. The initial inflection of the current trace during the ramp does not differ significantly in the presence and absence of drug; although NPPB or DPC is present, it does not block at these voltages. However, the shape of the curve later in the ramp is deflected in a concentration-dependent manner. If the drug is approximately at equilibrium with its binding site throughout the ramp, the current change at each time point reflects the voltage dependence of block. We can quantitate the development of block by fitting a first-order exponential function to the current trace to obtain a dimensionless value, ω, which is inversely proportional to the curvature of the current trace. The residual errors obtained with a first-order fit were small (standard deviation from the fit (σ) ~0.01), and were not improved by use of a second-order fit. As blockers are added, the curvature is increased, and the time-point (and, hence, voltage) at which the current trace flattens is reached earlier in the ramp, resulting in a decreased ω. Values of ω in the presence of drug can be normalized with respect to the values in the unblocked state (ω/ω_o).

One advantage of this analysis is that the ramp protocol can be run fairly fast relative to the protocol of multiple voltage steps used for steady-state analysis, allowing one to acquire data rapidly after brief solution changes. A second advantage is that the absolute value of ω in the absence of blockers is not affected by the magnitude of the unblocked current over a wide range of whole-cell conductances. Hence, blockade quantified by comparisons of I/I_o at −100 mV (steady-state analysis) for 100–200 μM DPC in WT-CFTR was more variable than blockade quantified by ω/ω_o (nonstationary analysis) for the same experiments, because the nonstationary analysis is much less sensitive to channel rundown than is steady-state analysis.

Analysis of Single-Channel Block

For single-channel measurements, digitized Fetchex records were analyzed using the Igor Pro version 3.11 (Wavemetrics; Lake Oswego, OR). Transition analysis used a 50% cutoff between the open and closed current levels. Open- and closed-time histograms were constructed with a bin width of 0.1 msec. For closed-time histograms, fitting began with the bin between 0.3 and 0.4 msec, which was the first bin past the system dead time. Time constants were taken from the fits to the histogram constructed for each patch. It should be noted that the brief closures observed in channels in the absence of drug are characterized by a time constant below the experimental resolution; hence, these values are actually extrapolated time constants. To calculate affinity at the single-channel level, it was necessary to correct the closing rates in the presence of drug ($1/\tau_o$) for the endogenous flicker observed in the absence of drug, as described [4]. The single-channel affinity was then calculated according to the following equation:

$$K_D^{(s\text{-}c)} = k^{-1}/k^1 = \{ (1/\tau_{C2}) / (1/\tau_o) \} [\text{drug}] \quad (3)$$

where τ_{C2} is the time-constant of the drug-induced closed state and τ_o is the corrected open time-constant in the presence of drug. The average on- and off-rates from multiple experiments were used to calculate one mean value for $K_D^{(s\text{-}c)}$.

Burst Analysis

Dwell time analysis of open bursts was performed using Igor software. Open bursts were defined as intervals separated by closings of 80 msec or greater, a value previously established to discriminate between ATP-dependent gating and intraburst blockade of CFTR in mammalian cells [67]. Since none of the intraburst closed time constants we measure

were even 5% of this 80 msec value, this is likely also a valid way to separate events reflecting ATP-dependent gating from events reflecting intraburst blockade of CFTR in oocytes. All recordings used in the analysis contained no more than three simultaneous open levels. For the multiple-channel recordings the mean burst duration was estimated using the following formula: $t_n = \sum_j \cdot t_j / n$, where t_j is the time the j channels are simultaneously open and n is the total number of transitions from an open burst to a interburst closed state. Thus, the multiple-channel open burst event is transformed to n single-channel open events with burst duration t for each event. This method was first described by Fenwick [13] and has been used in similar types of analysis of muscarinic K^+ channels [21] and more recently, CFTR [59].

Statistics

Unless otherwise noted, values given are mean ± SEM. Statistical analysis was performed using the *t*-test for unpaired measurements by SigmaStat (Jandel Scientific; San Rafael, CA) with $P \leq 0.05$ considered indicative of significance. Most figures include error bars; these are only visible when they exceed the size of the symbols.

Source of Reagents

Unless otherwise noted, all reagents were obtained from Sigma Chemical (St. Louis, MO). NPPB (5-nitro-2-(3-phenylpropylamino)-benzoate) was from Research Biochemicals International (Natick, MA); DPC (*N*-phenylanthranilic acid) was from Aldrich Chemical (Milwaukee, WI); L- 15 media was from Gibco/BRL (Gaithersburg, MD). NPPB and DPC were dissolved in DMSO at stock concentrations of 0.1–0.5 M. The final concentration of DMSO varied up to a maximum of 0.1%, which had no effect on ISO-activated currents.

Results

Rapid Block by Arylaminobenzoates

Expression of CFTR in oocytes and exposure to ISO led to the development of a chloride current that peaked within six to seven minutes. CFTR macroscopic currents were time-independent and exhibited mild outward rectification (Fig. 1). As shown previously [33], blockade of CFTR by arylaminobenzoates is fast and clearly voltage-dependent. Bath application of 100 μM NPPB or DPC to oocytes led to a voltage-dependent block of cAMP-activated current (Fig. 1*B* and *C*) over the course of several minutes. Six to seven minutes of incubation in the presence of bath-applied drug were required to achieve stable block of CFTR holding currents. Once this was achieved, the macroscopic blocking and unblocking kinetics of NPPB and DPC following steps to hyperpolarizing and depolarizing voltages, respectively, were rapid, resulting in time-independent blockade and relief from block (Fig. 1). Block by NPPB exhibited a voltage dependence similar to that of DPC block of steady-state currents under identical conditions (Fig. 2; $\Theta = 0.35 \pm 0.01$ and 0.37 ± 0.01, respectively ($P = 0.261$)), assuming an effective valence of 1.0 for each drug [33, 58], although block by NPPB was more efficacious than block by DPC. The apparent K_D (calculated using Eq. (1)) for WT-CFTR channels at pH 7.5 and $V_m = -100$ mV in the presence of 100 μM drug was 87.2 ± 3.4 μM and 201.4 ± 11.3 μM for NPPB and DPC, respectively (Table 1).

Block of Wild-type Single CFTR Channels by NPPB

To determine the mechanism of block at the single-channel level, WT-CFTR channels were studied in excised, inside-out patches, in the absence of drug and in the presence of 5 μM or 25 μM NPPB, at $V_m = -100$ mV. Sample current traces are shown in Fig. 3; Table 2 summarizes the intraburst kinetic features of WT channels in the presence and absence of NPPB. Blockade was not evident at depolarizing potentials (*not shown*), consistent with the voltage-dependence observed for block of macroscopic currents. For all analysis presented here, we describe the results for currents at $V_m = -100$ mV. Open-time histograms with and without drug were fit with a single exponential (Fig. 3*C* and *E*); in paired experiments, τ_o was reduced 2-fold by 5 μM NPPB and 4-fold by 25 μM NPPB. Closed-time histograms were fit with a single exponential in the absence of drug, but with a double exponential in the presence of NPPB (Fig. 3*D* and *F*). The brief, flickery closures evident in the absence of drug likely represent block by the pH buffer included in the intracellular solution for excised patch experiments [18, 22, 50]. Consistent with our previous results [33], this endogenous state was characterized by a time-constant, τ_{C1}, of approximately 0.2 msec. In the presence of NPPB, a second, tenfold longer time-constant, τ_{C2}, also contributed to the fit. In this regard, NPPB block of WT-CFTR channels resembled more closely the block of these channels by FFA than their block by DPC [33]. As expected for a bimolecular reaction between drug and receptor, the blocking rate, $1/\tau_o$, was dependent upon NPPB concentration, but the rate of the reverse reaction, $1/\tau_{C2}$ was not (Fig. 4*A*). Using data combined from multiple patches, the calculated affinity for NPPB block of single WT-CFTR channels was 35 μM.

Mechanism of Block

Although the results described above for NPPB, and described previously for DPC and FFA, are consistent with a simple pore-blockade, questions remain in the literature regarding the mechanism of action of arylaminobenzoates. Hence, we addressed this issue in three sets of experiments. First, we tested the effect of drug on open-channel burst duration. A defining characteristic of

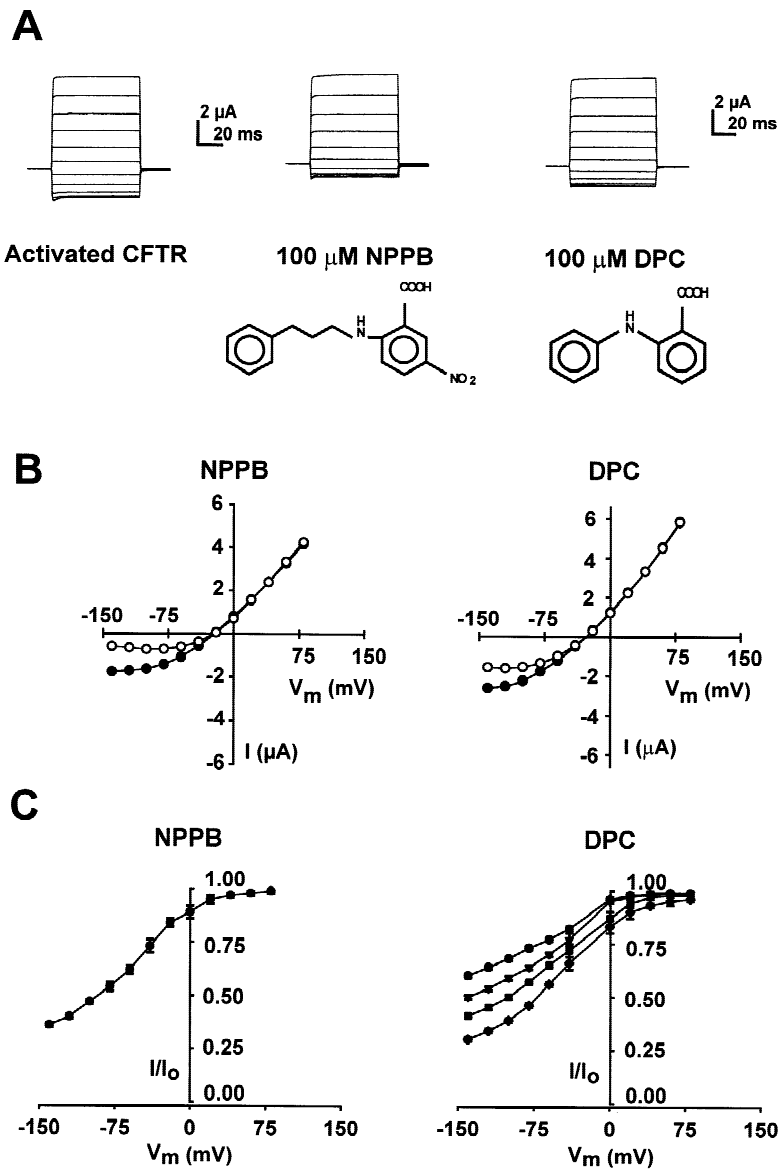

Fig. 1. Voltage-dependent block of the WT channel by NPPB and DPC. (*A*) Families of currents in the absence of drug (*left*) and presence of 100 μM NPPB (*center*) or 100 μM DPC (*right*). Voltage was stepped from a holding potential of −30 mV to test potentials between −140 and +80 mV at increments of +20 mV. CFTR currents were isolated by subtraction of background currents. Structures for NPPB and DPC are also shown. For experiments with NPPB, all solutions contained 1 mM $BaCl_2$ to limit activation of endogenous oocyte channels. (*B*) Current-voltage relation for one oocyte in the absence (*filled symbols*) and presence (*open symbols*) of 100 μM drug. (*C*) Fractional currents remaining in the presence of 100 μM NPPB (*left*) or various concentrations of DPC (*right*). I/I_o was calculated at all potentials from currents such as those shown in part (*A*). Concentrations used were: 100 μM (*circles*), 200 μM (*triangles*), 300 μM (*squares*), and 500 μM (*diamonds*). Mean ± SD for n = 5–6 oocytes at each concentration.

open-channel block is the lengthening of channel bursts due to the presence of drug in the pore, which prohibits channel closure [20]. The burst duration is lengthened in proportion to the time the channel spends in the open-but-blocked state. However, this has not been tested for block of CFTR by NPPB or any other arylaminobenzoate. By making use of the ability to control channel number in our oocyte expression system, we analyzed the open bursts in our recordings containing 1–3 channels, using a minimal interburst discriminator of 80 msec, a value previously determined to approximate the minimum duration of closures between bursts in unblocked channels undergoing normal gating by ATP hydrolysis [67]. NPPB increased the open-burst duration (τ_B) of WT-CFTR channels from a mean of 1553 ± 75 msec in the absence of blocker (n = 547 bursts) to 2433 ± 355 msec in the presence of 25 μM NPPB (n = 84 bursts; P = 0.001) (Fig. 4*B*). This is consistent with an open-channel block mechanism for NPPB, wherein the channel conformation is held in its open state, albeit blocked, by the occupancy of drug at its binding site.

Secondly, we asked whether DPC inhibits CFTR currents through an allosteric mechanism, which may be exhibited as inhibition of PKA-mediated activation. As shown in Fig. 5*A*, exposure to 200 μM DPC before ISO did not affect the time-course of activation. In this experiment, whole-cell conductance was calculated every 15 sec by stepping the membrane potential between +50 and −50 mV. Although the absolute plateau conductances differed in the presence and absence of drug (e.g., 62 *vs.* 85 μS with and without DPC, respectively), the time-course of development of the normalized conduc-

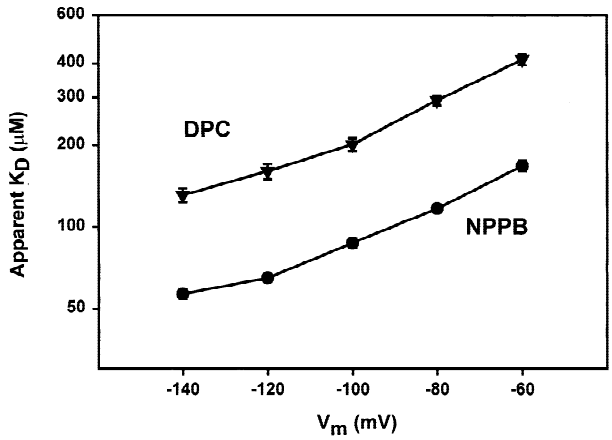

Fig. 2. Voltage dependence of blocker affinity in the WT channel at pH 7.5. Points are averages (±SE) from 5 oocytes for NPPB (*circles*) and 6 oocytes for DPC (*triangles*). The apparent K_D was calculated using Eq. 1, and plotted on a semilogarithmic scale as a function of voltage. The slope of the regression line (*not shown*) is proportional to the electrical binding distance, θ.

tance was not slowed by DPC; at no time-point was there a significant difference in the magnitude of the normalized conductance in the presence of DPC compared to in its absence. Similar results were obtained with NPPB (*not shown*). It is true that a decrease in whole-cell current, as described here, could arise from an effect of drug on the number of channels capable of opening, which would be consistent with allosteric inhibition. However, two observations argue against allosteric inhibition. First, the rapid kinetics of block at the single-channel level indicate that NPPB and DPC do not decrease the number of activated channels in a patch by constant inhibition of a fraction of the channels, but instead transiently inhibit all channels present in the patch during a fraction of their open times. Secondly, in comparisons of well-separated bursts from three recordings containing a single active CFTR channel in the presence or absence of NPPB, we found no evidence for an increase in interburst duration (a decrease in bursting rate), which would imply allosteric inhibition. These results are consistent with the notion that the mechanism of action of DPC and NPPB is simple pore blockade, without other allosteric effects on channel function.

Finally, the number of arylaminobenzoate binding sites on CFTR is unknown. A DPC dose-efficacy relationship was obtained by comparing the blocking effects at $V_m = -100$ mV of various bath [DPC] (Fig. 5*B*). This relationship could be fit best with a Hill equation yielding a Hill coefficient of 0.91 and a K_D of 278.0 ± 16.6 μM. This value is very similar to the mean K_D of 281.0 ± 19.5 μM calculated using Eq. (1) for each bath [DPC] at $V_m = -100$ mV. A Hill coefficient near unity suggests that a single binding site is responsible for the inhibition of CFTR currents by DPC. This is consistent with the homogeneous distribution of open times and of drug-induced closed times in single channel records. From these experiments, we conclude that DPC, and most likely the other arylaminobenzoates, block WT-CFTR by an open-channel mechanism via inhibition of ion flow by binding at one site in the pore of the channel, without affecting regions of the protein involved in channel activation. The notion that there is a single class of binding sites for NPPB is supported by: (i) a voltage-dependence of block identical to that of DPC, which blocks macroscopic currents with a Hill coefficient near unity; (ii) the presence of a single class of NPPB-induced closed times, indicating a homogeneous class of off-rates, consistent with a homogeneous class of drug-channel interactions; and (iii) the linear relationship between inverse open time and drug concentration, indicating a homogeneous population of on-rates at a given concentration.

Block by DPC and NPPB is pH-dependent

Our previous experiments with DPC showed that block of whole-cell CFTR currents was slow upon bath application, consistent with a mode of action requiring the drug to enter the channel pore from the cytoplasmic side [33]. The delayed block may arise from the time needed for drug diffusion across the membrane leading to accumulation of drug at an effective concentration in the cytoplasm. NPPB and DPC are hydrophobic molecules with only one ionizable group in each case, and pK_a values in the range of ~4 [51, 60]. Protonation of the carboxylate moiety at low pH would increase the hydrophobicity of the molecule, which should promote permeation through the membrane and accumulation of the drug in the cytoplasm. We tested this hypothesis by investigating the effect on CFTR blockade of altering the bath pH.

Whole-cell CFTR currents in the absence of blocker were not obviously affected by changes in bath pH. Steady-state currents at pH 6.5 and 8.0 resembled those at pH 7.5 in all respects, including mildly outwardly rectifying *I/V* relation and lack of time-dependence (Fig. 6). Incubation at bath pH 6.5 for several minutes induced a slight increase in rectification at strongly hyperpolarizing potentials. Whole-cell conductances (calculated between 0 and +80 mV) did not differ significantly: 46.0 ± 3.7 μS, 47.1 ± 3.8 μS, and 46.2 ± 3.7 μS for pH 6.5, 7.5, and 8.0, respectively ($n = 5$ each; $P > 0.8$). No effects on the activation rate were apparent following changes in bath pH.

Incubation with DPC or NPPB at reduced pH leads to improved steady-state blockade, in part due to enhanced loading of the hydrophobic drugs into the cytoplasm of the oocyte (Fig. 6; Table 1). In these experiments, bath pH was either held at 6.5, 7.5, or 8.0 during

Table 1. Affinity and voltage dependence for block by NPPB and DPC

Bath pH	Construct	NPPB			DPC		
		$K_D(-100)$ (μM)	Θ	*n*	$K_D(-100)$ (μM)	Θ	*n*
	WT	87.2 ± 3.4[a]	0.35 ± 0.01	5	201.4 ± 11.3	0.37 ± 0.01	6
7.5	S341A	287.7 ± 19.3[b,c]	0.38 ± 0.01[c]	5	1553.9 ± 121.0[a]	0.47 ± 0.01[a]	4
	T1134F	83.3 ± 3.9[d]	0.17 ± 0.01[b,d]	5	123.8 ± 9.2[a]	0.39 ± 0.01	4
	WT	50.1 ± 2.9	0.24 ± 0.01[f]	4	124.6 ± 7.2	0.27 ± 0.01[f]	5
6.5[e]	S341A	72.8 ± 4.5[b]	0.26 ± 0.01[f]	5	379.3 ± 21.1[a]	0.51 ± 0.01[a,g]	4
	T1134F	41.8 ± 4.0	0.14 ± 0.01[b,f]	4	40.3 ± 3.8[a]	0.29 ± 0.01[a]	5

Affinity for NPPB and DPC were determined empirically at −100 mV from whole-cell currents measured in the presence of 100 μM drug; for pH 6.5 experiments, [NPPB] was reduced to 50 μM. Θ is expressed as the fractional distance from the intracellular end of the pore. For these experiments, the slope was calculated from the $K_D(V)$ values over the range of −140 to −60 mV. Values given are mean ± SEM for *n* oocytes.

[a] $P < 0.01$ compared to WT block by DPC at the same pH.

[b] $P < 0.01$ compared to WT block by NPPB at the same pH.

[c] $P < 0.01$ compared to block of S341A-CFTR by DPC.

[d] $P < 0.01$ compared to block of T1134F-CFTR by DPC.

[e] All $K_D^{(-100)}$ values for NPPB and DPC at pH 6.5 are significantly different ($P < 0.01$) from the respective values at pH 7.5.

[f] $P < 0.01$ compared to Θ for equivalent experiments at pH 7.5.

[g] $P < 0.05$ compared to Θ for equivalent experiments at pH 7.5.

both drug loading and channel activation. (At pH 6.5, blockade by 100 μM NPPB was so great that inward currents were not observed, even at strongly hyperpolarizing potentials. Hence, it was necessary to reduce the [NPPB] to 50 μM for these experiments. As shown previously for DPC [33], plots of apparent K_D *vs.* voltage are independent of drug concentration for concentrations around the IC_{50}.) Drug was added for 1.5 min before activation with ISO. Loading at pH 6.5 resulted in a reduced apparent K_D at all voltages (Table 1). For both drugs, $K_D^{(-100)}$ at pH 6.5 was only ~60% that at pH 7.5 ($P < 0.001$ in each case). These results are consistent with an effect of pH upon the effective concentration of drug in the cytoplasm. Similar results have been reported for block of cardiac CFTR by NPPB and its congeners [58].

Aside from this indirect effect of pH on block by arylaminobenzoates, we reasoned that there may also be direct effects of changing the bath pH. Hence, we asked whether changing the bath pH altered parameters other than those sensitive to the extent of drug loading. The steady-state voltage dependence of blockade of the WT channel by NPPB was sensitive to bath pH; $\Theta = 0.35 \pm 0.01$ and 0.24 ± 0.01 at pH 7.5 and 6.5, respectively ($P < 0.001$). Low bath pH also shifted the voltage dependence for block by DPC; $\Theta = 0.37 \pm 0.01$ and 0.27 ± 0.01 at pH 7.5 and 6.5, respectively ($P < 0.001$; Table 1). This shift in voltage dependence of steady-state block implies that amino acids with protonatable side-chains may be located in or near the binding region for DPC and NPPB.

To distinguish between direct and indirect pH-dependent effects on blocker efficacy, we also made use of a protocol that allows rapid quantitation of voltage-dependent blockade immediately following changes in bath solution. Hence, block of CFTR currents in oocytes was also quantitated using nonstationary analysis (*see* Materials and Methods). This analysis involves quantitation of the degree of block by measurement of the drug-induced curvature in CFTR currents during a hyperpolarizing ramp (Fig. 7*A*) to calculate a value, ω, which is inversely proportional to the magnitude of block. cAMP-activated currents measured using this protocol exhibited inhibition by NPPB or DPC at concentrations as low as 10 μM, leading to reduced values of ω. Because the membrane potential was depolarized before the beginning of the ramp, the curvature induced in the current trace at hyperpolarizing potentials represents the developing interaction between the drug and its receptor. This voltage-dependent interaction is not likely to be due to drug entering and exiting the pore via the membrane lipid: the fast rate of block during the 50 msec ramp is inconsistent with the longer time required for drug to re-equilibrate through the membrane phase to result in a significant change in cytoplasmic concentration.

ω values in the presence of drug can be normalized to values in the absence of drug to yield ω/ω_o. For these experiments, oocytes were activated by ISO for 6–7 min in the presence of DPC at the concentrations shown. As expected, the calculated ω/ω_o is dose-dependent. A plot of ω/ω_o *vs.* $[DPC]_{bath}$ reveals an exponential relationship

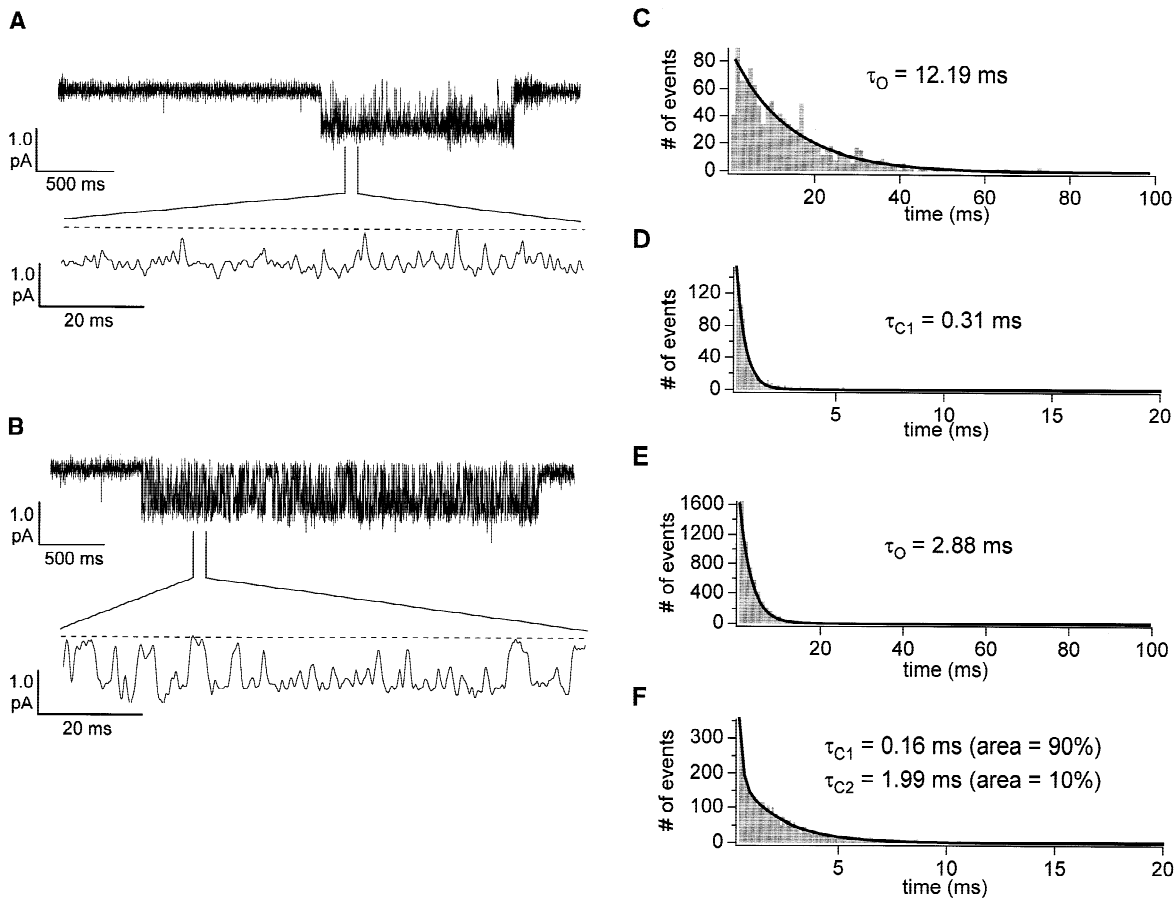

Fig. 3. Effect of NPPB at the cytoplasmic face of excised, inside-out patches expressing WT-CFTR channels. (*A* and *B*) Current traces in the absence and presence of 25 μM NPPB, respectively, at $V_m = -100$ mV. The data were filtered at 1 kHz and acquired at 5 kHz. The top traces in (*A*) and (*B*) represent ~3 sec of recording. Bottom traces in each case represent 100 msec. The dashed line in the expanded trace marks the closed current level. (*C* and *D*) Representative open- and closed-time histograms for a channel in the absence of drug. (*E* and *F*) Representative open- and closed-time histograms for a channel in the presence of 25 μM NPPB. The solid line represents the fit to a single exponential (*C-E*) or a double exponential (*F*). In (*F*), "area" represents the contribution to the fit from each component of the closed-time histogram. Mean values for these kinetic parameters are given in Table 2.

(Fig. 7*B*). Greater efficacy of blockade by NPPB compared to DPC was shown using nonstationary analysis as well as using steady-state analysis. ω/ω_o for 100 μM NPPB at pH 7.5 in WT was 0.39 ± 0.02 ($n = 4$). In contrast, this value for DPC was 0.56 ± 0.01 ($n = 10$; $P = 0.005$) at pH 7.5.

Absolute values of ω for currents in the absence of blocker were not affected by bath pH: 56.7 ± 2.1, 59.2 ± 1.3, and 58.5 ± 4.1 for pH 6.5, 7.5, and 8.0, respectively ($n = 5$ each; $P > 0.2$). However, consistent with an effect on drug loading, decreasing pH from 7.5 to 6.5 resulted in a leftward shift in the ω/ω_o *vs.* [DPC] curve (Fig. 7*B*). Increasing bath pH to 8.0 resulted in an rightward shift. Low pH also enhanced blockade by NPPB according to this analysis (*not shown*).

To differentiate between effects of bath pH on drug loading and more direct effects on drug-protein interaction, we asked whether the characteristics of block by DPC were affected by rapid changes in bath pH. ω/ω_o values for cells loaded and assayed in the presence of 200 μM DPC at pH 6.5, 7.5, and 8.0 are compared in Fig. 8 (Protocol #1). When cells were loaded with DPC (200 μM) at pH 6.5 for 7 min, then exposed for one minute to pH 7.5 in the continuing presence of drug, the degree of block was relieved as shown by an increase in ω/ω_o (Protocol #2, Fig. 8). This most likely represents a direct effect on drug block, rather than due to a change in the cytoplasmic [DPC] during the brief exposure to elevated bath pH; because drug loading into the cytoplasm requires several min, it is unlikely that the intracellular DPC concentration had changed drastically during the 1-min exposure to pH 7.5. Changes in cytoplasmic pH in oocytes during recovery from acid load are slow [2], suggesting that these results are not due to a change in the protonation state of cytoplasmic DPC. Furthermore, because the bath pH was shifted between two and three

Table 2. Kinetics of single-channel block in excised patches at $V_m = -100$ mV

CFTR Variant	[NPPB] (μM)	τ_O (msec)	τ_{C1} (msec)	τ_{C2} (msec)	Area τ_{C2} (%)	*n*	*T* (*sec*)
WT	0	8.93 ± 1.38	0.24 ± 0.02			7	415
	5	4.12[a] ± 0.32	0.23 ± 0.01	2.07 ± 0.14	2.5	4	216
	25	2.40[a,b] ± 0.28	0.29 ± 0.06	2.35 ± 0.47	10.8[b]	4	238
T1134F	0	17.63 ± 1.68	0.31 ± 0.05	1.33 ± 0.13	3.0	3	160
	5	8.46[a] ± 0.59	0.49[a] ± 0.03	3.14[a] ± 0.24	3.3	3	156
	25	5.72[a,b] ± 0.27	0.63[a] ± 0.10	2.82[a] ± 0.45	18.3[a,b]	3	174

[a] $P < 0.05$ Compared to unblocked channels.
[b] $P < 0.05$ Compared to channels in the presence of 5 μM drug.
n Number of patches.
T Total time, in seconds, for each condition.

pH units above the pK_a for DPC, the change in the amount of uncharged drug in the bath was small. This conclusion that this represents a direct effect of pH is also supported by the finding that only after prolonged exposure to elevated bath pH did ω/ω_o increase further, consistent with relief of blockade by reduction in the cytoplasmic [DPC] (*not shown*). Finally, ω/ω_o after loading at pH 6.5 and brief exposure to pH 7.5 was significantly greater than the value calculated when oocytes were loaded and assayed at pH 7.5 ($P < 0.01$; compare gray bars in Fig. 8). Hence, block by DPC exhibited a different dependence upon bath pH when the effects of pH upon drug loading were accounted for; the difference between the results from these two protocols suggests that pH affects more than just the loading efficiency of the drugs.

Pore-Domain Mutations Differentially Affect Block by DPC and NPPB

We have shown previously that mutations S341A and T1134F decrease and increase, respectively, affinity for DPC at −100 mV [35]. Loss of the binding site at S341 also shifted the voltage dependence for block of CFTR by DPC. The data reported here indicate that the voltage-dependencies for blockade of the WT channel by NPPB and DPC at pH 7.5 are approximately equal (Table 1). Block by both drugs was reduced in S341A-CFTR (Fig. 9*A* and *C*). However, both S341A-CFTR and T1134F-CFTR responded differently to block by NPPB and DPC. Mutation S341A-CFTR altered the voltage-dependence for block by DPC but not for block by NPPB. Similarly, instead of changing the affinity for NPPB, as was shown for DPC, T1134F-CFTR reduced the voltage dependence for NPPB (Fig. 9*A*, Table 1). The order of sensitivity for block by NPPB at −100 mV was T1134F = WT > S341A.

Low pH treatment (during drug loading and assay) did not shift the order of sensitivity between WT, S341A-CFTR, and T1134F-CFTR for block by DPC (Fig. 9*D*). However, the voltage-dependencies for block by DPC of WT and these two indicator mutations were affected by low bath pH. For WT and T1134F-CFTR, the voltage dependence for block by DPC was decreased at pH 6.5 ($P < 0.001$). In contrast, the voltage dependence of block of S341A-CFTR was increased at pH 6.5 ($P = 0.038$). Low bath pH also changed both the relative efficacy and voltage dependence for block by NPPB of WT and these two mutations (Fig. 9*B*, Table 1). For WT, S341A-CFTR, and T1134F-CFTR, the voltage dependence for block by NPPB was decreased at pH 6.5.

Blockade of Single T1134F-CFTR Channels by NPPB

Our recordings of macroscopic CFTR current indicated that mutation T1134F-CFTR affected block by NPPB and DPC in different ways: the mutation increased the affinity at −100 mV for DPC without changing voltage-dependence [35], but decreased the voltage-dependence of block by NPPB without changing the affinity at −100 mV (Table 1). To determine the basis for this discrepancy, we turned to analysis of single T1134F-CFTR channels. We have shown previously that T1134F-CFTR channels in the absence of blocker exhibit kinetics somewhat divergent from those of WT-CFTR channels. First, single-channel amplitude is decreased by ~28% [35]. Secondly, open time-constants were somewhat longer in the mutant (Table 2). More importantly, unblocked T1134F-CFTR channels exhibit two closed time-constants compared to only one seen in WT-CFTR (Fig. 10). The shorter closed duration likely represents buffer block, as described above for WT channels; the extra endogenous closed time constant, averaging 1.33 msec in duration, may arise from insertion of the phenylalanine side chain into the permeation pathway. Both of these time-constants, τ_{C1} and τ_{C2}, were roughly doubled in the presence of 5 or 25 μM NPPB (Table 2).

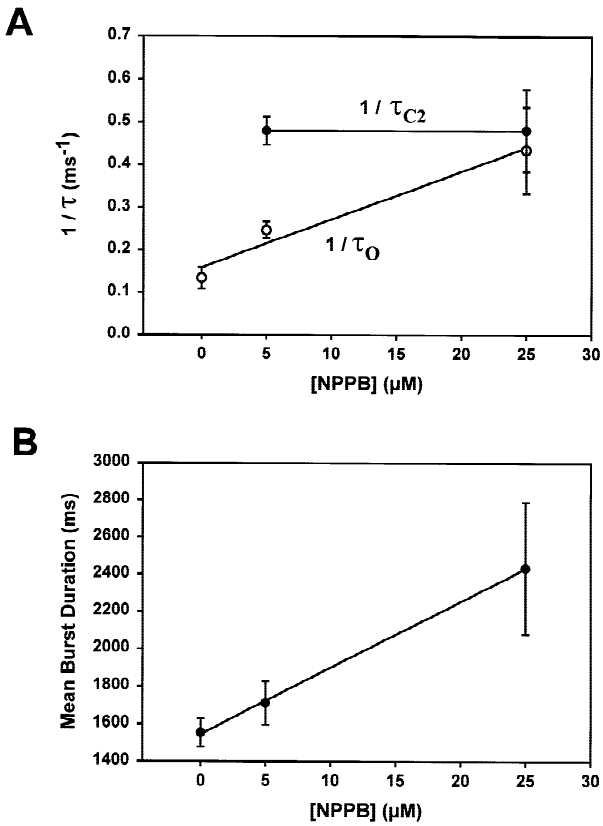

Fig. 4. Dose-dependence of the effects of NPPB on kinetics of single-channels in WT-CFTR. (*A*) Effect of drug concentration on closing rate (*open circles*, $1/\tau_O$) and opening rate (*filled circles*, $1/\tau_{C2}$). The horizontal line represents the average of $1/\tau_{C2}$ for 5 and 25 μM NPPB. The sloped line is the regression line for values of $1/\tau_O$. Note that the closing rate increases with [NPPB], while the opening rate is concentration-independent, as predicted from the bimolecular interaction of the drug with the channel. (*B*) Evidence that NPPB is an open-channel blocker. Well-separated bursts in recordings from patches expressing a limited number of WT-CFTR channels were analyzed in the absence of drug and in the presence of 5 or 25 μM NPPB. Burst duration was increased in a concentration-dependent manner from 1553 ± 75 msec (n (number of bursts) = 547) to 1710 ± 115 msec (n = 93) and 2433 ± 355 msec (n = 84) for 0, 5, and 25 μM NPPB, respectively ($P < 0.001$ for 0 *vs.* 25 μM). The line shown is the regression line.

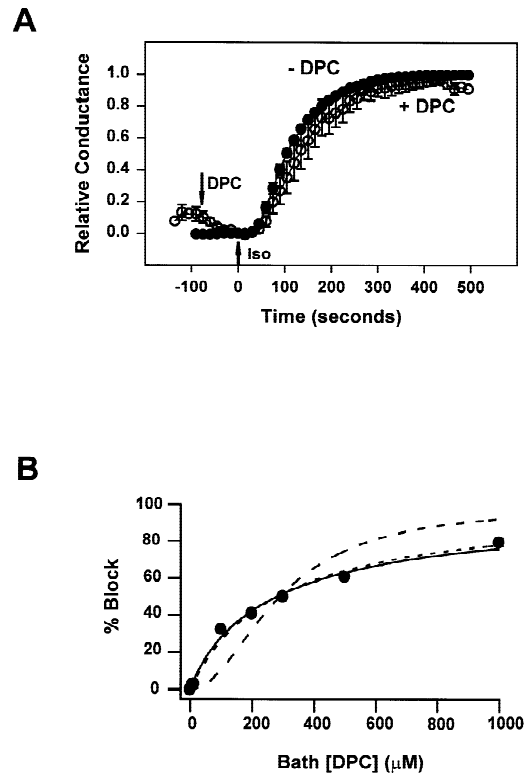

Fig. 5. Arylaminobenzoates inhibit CFTR by a simple pore-block mechanism. (*A*) DPC does not affect activation of CFTR. The development of conductance after treatment with ISO was measured through time by stepping the membrane potential to −50 and +50 mV every 15 sec. Conductance at each observation in the presence (*open symbols*) or absence (*filled symbols*) of DPC was set relative to the peak conductance. Exposure to 200 μM DPC did not affect the overall time course of activation. Each point is mean ± SD for n = 9 oocytes. (*B*) Concentration dependence of block by DPC suggests one binding site. Fractional block of macroscopic currents at −100 mV was plotted as a function of [DPC]. The point at 1 mM [DPC] is from a previous report [33]. The data were fit with three different functions: an unrestricted Hill equation (*solid line*) which yielded a K_D of 278.0 ± 16.6 μM and a Hill coefficient of 0.91; and two modified Hill equations in which the Hill coefficients were set to one (*short dashed line*) and two (*long dashed line*). A K_D of 279.6 ± 16.0 μM was obtained from the data when the Hill coefficient was set to 1, while the data could not be fitted properly using a Hill coefficient of two. This suggests that DPC inhibits CFTR by binding at a single site.

The distinction between τ_{C2} values in the absence and presence of NPPB was not large enough to require adjustments to the fit. However, as drug concentration was increased, the longer blocked state (τ_{C2}) contributed more events to the closed-time histograms, indicating that this is the primary drug-induced closed state. The increase in the duration of the shorter blocked state (τ_{C1}) in the presence of drug may represent stabilization of the buffer block by the presence of NPPB at its binding site.

Using data combined from multiple patches, the affinity ($K_D^{(s\text{-}c)}$) for NPPB of single T1134F-CFTR channels at −100 mV was calculated to be 75 μM, compared to 35 μM for WT-CFTR. In contrast, the affinity for DPC was increased in T1134F-CFTR channels: $K_D^{(s\text{-}c)}$ for DPC was 175 μM for WT-CFTR [33] and 88 μM in T1134F-CFTR [35]. The reduction in single-channel affinity for NPPB in the mutant may arise from the shift in voltage-dependence evident in block of macroscopic currents. The relationship between apparent affinity and voltage in block of macroscopic currents for WT and the mutant cross at −100 mV (Fig. 9*A*). This relationship could easily be altered by the difference between the concentration of Cl^- in our solutions for excised patch experiments and the intracellular Cl^- concentration in the intact oocyte. In the whole-cell experiments, the K_D is

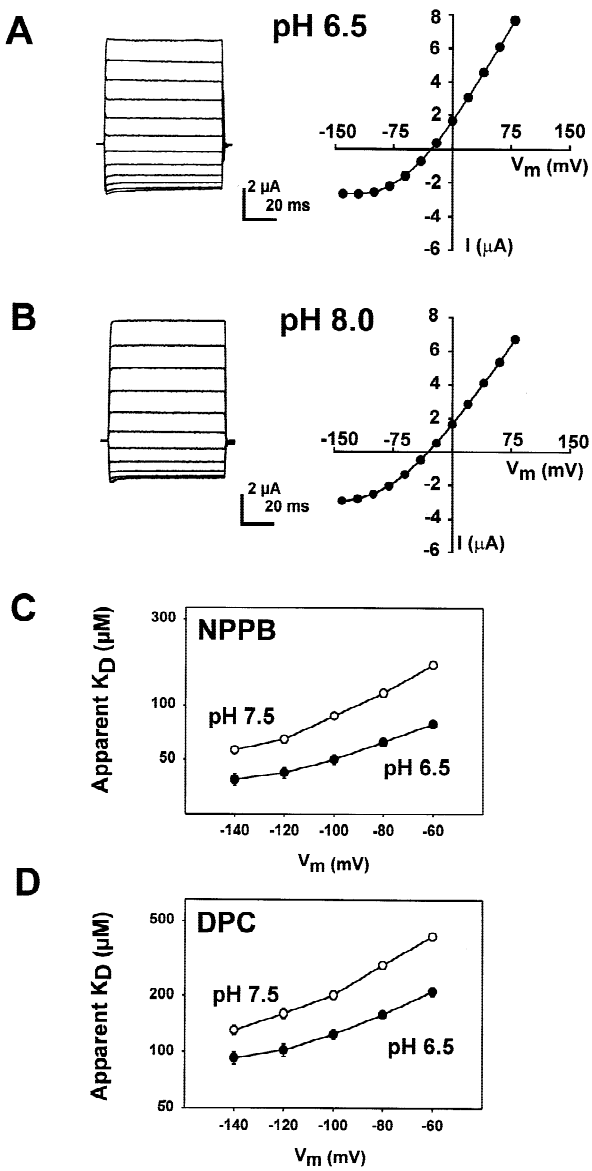

Fig. 6. Effects of bath pH on block by NPPB and DPC. (*A* and *B*) Whole-cell CFTR currents are not highly sensitive to bath pH. cAMP-activated currents were measured in separate cells at bath pH 6.5 (*A*) or 8.0 (*B*), using voltage protocols identical to those used for Fig. 1. No differences in time-dependence of macroscopic currents or linearity of current-voltage relations were observed, aside from a slight increase in Goldman rectification at strongly hyperpolarizing potentials at pH 6.5. (*C* and *D*) Affinity and voltage dependence of block are altered at low bath pH. Apparent affinity for NPPB (*C*) and DPC (*D*) was calculated as in Fig. 2, at either pH 7.5 (*open symbols*) or 6.5 (*filled symbols*). For experiments with NPPB at pH 6.5, drug concentration was 50 μM; for all others, drug concentration was 100 μM. Points are mean ± *SE* for $n = 5$–6 oocytes in each condition.

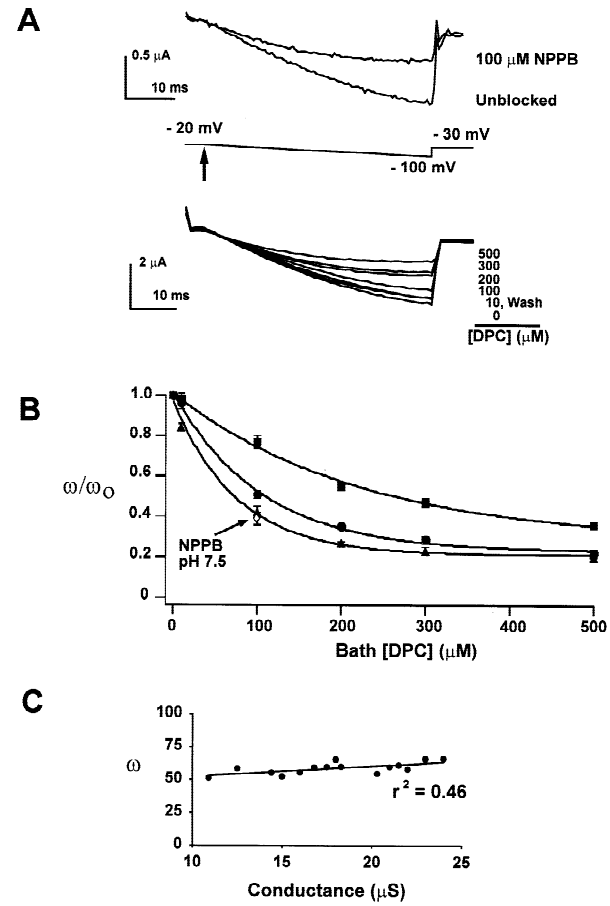

Fig. 7. Quantitation of block using nonstationary analysis. (*A*) Currents were measured from oocytes activated by ISO treatment in the presence or absence of NPPB (*top*) or DPC (*bottom*) at the bath concentrations shown. Membrane voltage was stepped to +40 mV for 465 msec (*not shown*), then to −20 mV for 5 msec, and then ramped to −100 mV over 50 msec (voltage protocol is shown in the middle of panel (*A*); *arrow* indicates initiation of the ramp). (*B*) An exponential function was fit to the current traces shown in part (*A*), to calculate a measure of the drug-induced curvature (ω). Values of ω in the presence of drug were set relative to the value calculated in the absence of drug to determine ω/ω_o. For DPC, ω/ω_o was calculated at the concentrations shown with the bath pH set to 8.0 (*squares*), 7.5 (*circles*), or 6.5 (*triangles*). The *open diamond* marks ω/ω_o calculated with 100 μM NPPB at pH 7.5. Points are mean ± SD for $n = 6$–10 oocytes in each condition. (*C*) The absolute value of ω in the absence of drug is not sensitive to the magnitude of the activated current. Conductance (between +80 and −140 mV) was calculated at 2, 4, and 6 min during activation of WT-CFTR upon exposure to ISO for $n = 5$ oocytes. Absolute value of ω averaged 58.9 ± 4.6 (mean ± SD) for these measurements, and was independent of whole-cell conductance ($r^2 = 0.46$).

calculated at −100 mV, representing only a 70 mV shift from the reversal potential of ~ −30 mV. For the patch experiments, with symmetrical [Cl^-], a clamp voltage of −100 mV represents a stronger driving force. This would be equivalent to a leftward shift from the crossover point in Fig. 9*A*, into a voltage range where the mutant is blocked less effectively than WT. Block of single S341A-CFTR channels was not studied, due to the low single-channel conductance of this variant [35].

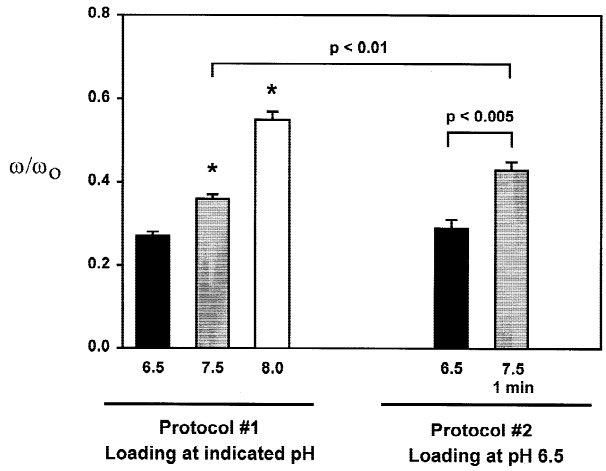

Fig. 8. Effects of rapid pH changes on block by DPC. (*Left*) Protocol #1: Cells were loaded with 200 μM DPC at the indicated pH for 1.5 min prior to and 6–7 min during activation of CFTR with ISO, and then assayed at that pH using nonstationary analysis to calculate ω/ω_O. (*Right*) Protocol #2: Cells were loaded with 200 μM DPC at pH 6.5 for 1.5 min prior to and 6–7 min during activation of CFTR. The degree of block was assayed at pH 6.5, then after 1 min exposure to DPC-containing solution at pH 7.5. Brief exposure to pH 7.5 caused relief of block to a significant degree. The degree of block at pH 7.5 (*gray bars*) measured with these two protocols differed significantly ($P = 0.004$). Bars show mean ± SD for $n = 5$–8 oocytes at each condition.

Discussion

Pharmacological agents that inhibit ion channels by blocking the pore have provided useful tools for the identification of and study of the permeation pathway in many types of ion channels [25]. In the case of potassium channels, high affinity probes in the form of peptide blockers such as charybdotoxin have enabled detailed analysis of the pore using a structure/function approach [31]; nonpeptide blockers, such as TEA, also serve as probes of the pore, albeit with lower affinity [66]. Conclusions derived from studies using both types of probes were validated when a canonical potassium channel pore-forming subunit was crystallized and studied at high resolution [11]. Unfortunately, peptide blockers of CFTR have not been described [41], so one must rely on the blockers available. Organic blockers, such as the arylaminobenzoates, do not exhibit affinity for CFTR as high as that of the peptide blockers of potassium channel pores. While their on-rates, measured in experiments such as those described here, are high, their off-rates are typically also high, indicating that there is not an intimate interaction between the organic blocker and the pore. However, we have shown, in this study and previously [35], that organic blockers may be used to derive information regarding the structure of the CFTR pore.

The arylaminobenzoates represent one of the most heavily studied classes of blockers of the CFTR Cl^-

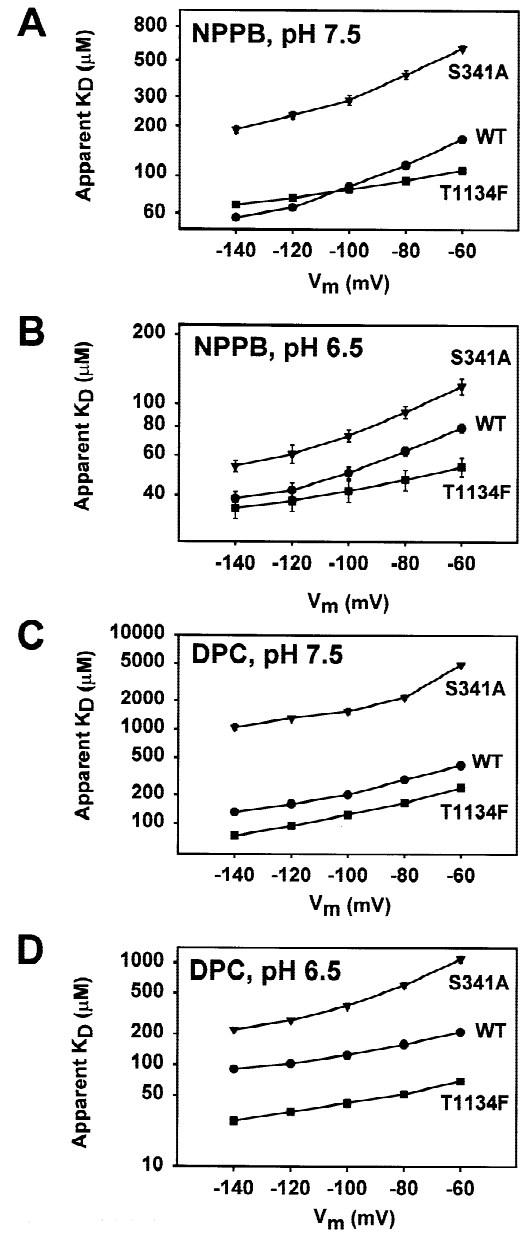

Fig. 9. Effects of pore-domain mutations on pH-dependent block. (*A* and *B*) Voltage dependence of NPPB affinity for wild-type and two mutations. Apparent affinity for NPPB was measured at pH 7.5 (*A*) and pH 6.5 (*B*) for WT (*circles*) and the two indicator mutations S341A-CFTR (*triangles*) and T1134F-CFTR (*squares*) which had previously been shown to decrease and increase, respectively, affinity for DPC. Drug concentration was 50 μM for pH 6.5 and 100 μM for pH 7.5. Data for WT, pH 7.5, are the same as those shown in Fig. 2 (*see* Table 1 for number of experiments). (*C* and *D*) Voltage dependence of DPC affinity for wild-type and two mutations. Apparent affinity for DPC was measured at pH 7.5 (*C*) and pH 6.5 (*D*) for WT (*circles*) and the two indicator mutations S341A-CFTR (*triangles*) and T1134F-CFTR (*squares*). Drug concentration was 100 μM in each case. Data for WT, pH 7.5, are the same as those shown in Fig. 2 (*see* Table 1 for number of experiments).

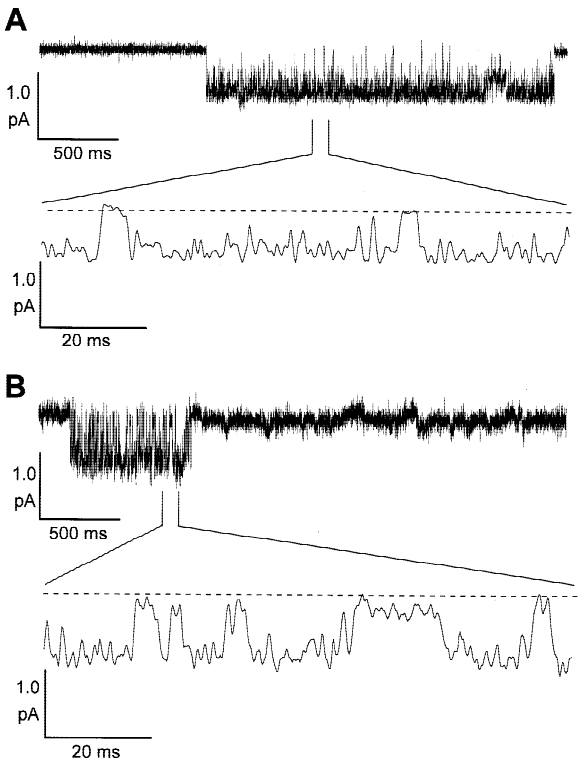

Fig. 10. Block of single T1134F-CFTR channels by NPPB. (*A* and *B*) Current traces in the absence and presence of 25 μM NPPB, respectively, at $V_m = -100$ mV. The top traces in (*A*) and (*B*) represent ~3 sec of recording. Bottom traces in each case represent 100 msec. The dashed line in the expanded trace marks the closed current level. Mean values for kinetic parameters in T1134F-CFTR channels are given in Table 2.

channel, but their mechanism of action is unclear; DPC is the only blocker of CFTR for which a binding site has been identified [35]. DPC was first developed as a blocker of the basolateral Cl^- conductance of rabbit thick ascending limb of the loop of Henle, and the apical Cl^- conductance of shark rectal gland tubules [9]. In an extensive study of structure/activity relationships (SAR) using 219 compounds, Wangemann and coworkers [60] showed that NPPB has enhanced efficacy over DPC and FFA. NPPB blocks CFTR expressed in many cell types. In cardiac cells, DPC and NPPB block CFTR with a roughly similar voltage dependence [57, 58]. Extension of the aliphatic chain beyond that of NPPB, to form 5-nitro-2-(4-phenylbutylamino)-benzoic acid (NPBA) did not improve efficacy of block of whole-cell currents in guinea pig cardiac myocytes [58] or in the epithelial form of CFTR expressed heterologously in oocytes [56]. Walsh and coworkers have recently investigated the structural determinants of affinity for the interaction between arylaminobenzoates and CFTR by testing the effects of chemical modifications on the structure of NPPB. They found that: (i) removal of the nitro group decreased potency; (ii) removal of the benzoate ring obliterated block; (iii) removal of the phenyl ring caused a small decrease in potency; and (iv) addition of another phenyl ring enhanced block threefold [56].

We have attempted to define further features of the mechanism of action of NPPB and DPC by studying their block of CFTR expressed in oocytes. The principal findings are these: (i) NPPB and DPC are voltage-dependent blockers with a mechanism most consistent with simple pore blockade. (ii) In direct comparison under identical conditions, NPPB is more efficacious than DPC, but has nearly identical voltage-dependence. (iii) In single-channel recordings, block by NPPB is evident by the appearance of a single class of drug-induced closed times. (iv) Block by NPPB and DPC is sensitive to bath pH; bath pH affects not only the extent of loading into the cell, but also alters the voltage-dependence of block. (v) Blockade by NPPB and DPC are differentially sensitive to mutations in putative pore-lining domains.

Mechanism of Block

Arylaminobenzoates block Cl^- channels in a wide variety of cells and tissues (for recent reviews, *see* [3, 17, 41]). Although the original studies using these compounds described significant block at very low concentrations (IC_{50} of 26 μM and 80 nM for DPC and NPPB, respectively), most investigators have used very high concentrations of DPC to identify the Cl^- currents of interest as being carried by CFTR [7, 30, 38, 54]. This is potentially problematic, because at high concentrations these drugs have side-effects such as inhibition of forskolin-stimulated cAMP production [19] and inhibition of prostaglandin synthesis in tracheal cells [14, 49]. Furthermore, inhibition by arylaminobenzoates of a variety of nonchloride ion channels has also been shown [6, 10, 16, 24, 36]. Hence, interpretations must be approached with caution in studies that use these drugs at high concentrations.

At the concentrations used in the present study, there was no evidence of an effect of DPC (or NPPB) pretreatment on the rate of activation of CFTR using the β_2-adrenergic receptor coexpression strategy (Fig. 5). Also, because outward currents are not inhibited by DPC even at concentrations well above the $K_D^{(-100)}$, despite prolonged incubation (Fig. 1*C*), there is no evidence of effects on any component of the signal-transduction pathway between the β-receptor and CFTR. Hence, it is unlikely that DPC and NPPB inhibit CFTR currents by disrupting the regulation of CFTR gating. In contrast, mutations in the cytoplasmic regulatory domain and nucleotide-binding domains of CFTR affect the activation rate and sensitivity to activating conditions, usually by alteration of the binding and hydrolysis of nucleotides [12, 47, 62].

Block of CFTR whole-cell currents by NPPB and DPC requires several minutes exposure to reach full effect [33], as if the drugs must cross the membrane to reach their binding sites. Due to the hydrophobic character of the arylaminobenzoates, investigators have expressed concern that they may inhibit CFTR by an allosteric effect at a site within the integral membrane domain, rather than by interrupting the flow of Cl^- through the aqueous pore. Indeed, the rapid development of steady-state block upon stepping to hyperpolarizing potentials and the immediate relief from block at depolarizing potentials leave one little opportunity to witness the binding and unbinding of DPC. This is, however, consistent with our previous kinetic measurements in excised patches [35], wherein the on-rate and off-rate at −100 mV were shown to be fast ($6.4 \times 10^6\ M^{-1}\ sec^{-1}$ and $560\ sec^{-1}$, respectively, for DPC block of T1134F-CFTR).

Block of WT-CFTR by three arylaminobenzoates (DPC, FFA, and NPPB) has now been studied at the single-channel level ([33, 35] and *present study*). All three drugs block from the cytoplasmic side, and only inhibit single-channels at hyperpolarizing potentials. In each case, single-channel records in the absence of drug exhibit an endogenous closed time of brief duration (~0.25–0.3 msec) that likely represents block by the pH buffer [18, 22, 50]. Application of drug to the cytoplasmic side of the patch results in the appearance of a longer closed state, representing inhibition of Cl^- permeation. The drug-induced closed times increase in duration in the same order as the potency for inhibition of macroscopic currents: 0.62 ms, 1.11 msec, and 2.35 msec for DPC, FFA, and NPPB, respectively. Hence, it appears that increased efficacy in this family of drugs arises, at least in part, from a decrease in off-rate.

For macroscopic block, the affinity for DPC at −100 mV calculated for each drug concentration studied gives an average K_D of 281 μM, with a dose-response relationship consistent with a single site of interaction. Although others have proposed two separate inhibitory effects of NPPB, one voltage-dependent and one voltage-independent [56], a Hill coefficient near unity confirms that CFTR has one class of DPC-binding sites, with distinct voltage-dependence. We assume that this is true for other arylaminobenzoates. Furthermore, the observation of a single drug-induced closed time (τ_{C2}) in patch experiments suggests a single class of binding sites for NPPB (*present study*) and for FFA [33]. These results are consistent with a mechanism of action by simple pore blockade.

Other data also support a pore-blocking mechanism, as follows. (i) The rapid flicker induced in CFTR single-channel records upon exposure to NPPB (*present study*) or DPC [33] resembles open-channel block described in other systems [20], wherein the flicker arises from the residence of the blocker on its site. (ii) Blockade is voltage-dependent; the direction of the voltage dependence is consistent with an apparent requirement that the drugs reach their binding sites after permeating the membrane to the cytoplasmic side of the channel, as shown by block of single channels in cell-attached mode after application of DPC to the extracellular medium [33]. (iii) Blockade is modulated by permeant anions, in a lock-in experiment where the efficacy of blockade is increased by a reduction in the extracellular concentration of permeant anion [35] or reduced by substitution of Cl^- by SCN^- as the permeant anion [56]. iv) NPPB increases the open-burst duration in a concentration-dependent manner. (v) Finally, kinetic analysis of blockade by NPPB or DPC indicated that the mean open-time for single CFTR channels was inversely related to drug concentration, while mean closed time was unaffected. These findings strongly support the notion that the arylaminobenzoates block within the pore and, therefore, may be useful as probes of pore structure.

Differential Sensitivity to Pore-Domain Mutations

We have shown previously that TM domains 6 and 12 contribute to the pore of the CFTR channel, based upon several observations. Mutations in both TM6 and TM12 affect single-channel conductance, rectification of current-voltage relations, selectivity among monovalent anions ([34], *see also* [27–29, 50]) and affinity and/or voltage dependence of block by DPC [35]. In general, mutations in TM12 were found to have weaker effects on permeation than similar substitutions in TM6, leading us to conclude that TM6 and TM12 make asymmetric contributions to permeation in this channel. Several mutations were found that affected neither affinity for or voltage dependence of block by DPC [35]. Hence, there is some specificity for use of this approach to identify sites that line the pore. We proposed that two cross-sectional domains within the pore could be described: a binding domain at the level of S341 in TM6 and S1141 in TM12, because mutations at this level had the largest effect on affinity and voltage dependence for block by DPC, and a modifying domain at the level of K335 and T1134, because mutations at this level affected only the affinity for DPC [35]. More recent studies suggest that TM5 ([32, 48]; and *unpublished observations*) and TM11 [69] also line the pore. Hence, our working model has TM domains 5, 6, 11, and 12 contributing to the walls of the pore in CFTR. Continuing this approach to structure-function studies in CFTR requires the availability of molecular probes that can be used to investigate different regions of the pore. We therefore asked whether DPC and NPPB experience the same regions within the pore, or might they show differences in their interactions between drug and protein.

In these experiments, under identical conditions, NPPB was more efficacious at blocking the WT channel than was DPC. The voltage dependence for DPC and NPPB block of the WT channel was essentially the same (Table 1), suggesting, but not necessarily proving, that the binding sites for these two drugs overlap in the voltage field. Consistent with our previous results, the order of sensitivity to DPC at −100 mV was as follows (Table 1): T1134F-CFTR > WT > S341A-CFTR. Block of T1134F-CFTR and WT-CFTR by DPC exhibited the same voltage dependence, while in S341A-CFTR the drug appeared to bind deeper in the pore (closer to the extracellular end). Block of CFTR by NPPB was impacted by these two mutations in different ways, compared to block by DPC. The order of sensitivity at −100 mV was: WT = T1134F-CFTR > S341A-CFTR. Most strikingly, the voltage dependence of block by NPPB was altered in a manner exactly the opposite to that of block by DPC. WT-CFTR and S341A-CFTR exhibited voltage dependencies that were not significantly different, while in T1134F-CFTR the drug appeared to bind less deeply within the pore (closer to the cytoplasmic end). Finally, while mutation T1134F altered the kinetics of block of single-channels by both DPC [35] and NPPB (*present study*), the effects of this mutation were not the same for the two drugs.

Our data show that while NPPB and DPC bind at very similar positions, their overall binding pockets are not identical. However, we reserve caution in concluding that the blockers interact directly with the sidechains at positions 341 and 1134. Allosteric effects of either mutation may have distinct actions on the two blockers simply due to structural differences between the blockers themselves. It is likely that the extended length of the NPPB molecule places the phenyl ring in closer apposition to the phenylalanine at T1134F, which may introduce electrostatic interactions that stabilize the drug at its binding site. Consistent with this hypothesis, the duration of τ_{C2} in the presence of NPPB was greater for T1134F than for WT. Further studies will be required to investigate this mechanism.

Walsh and coworkers have also studied the effects of pore-domain mutations on block by NPPB [56]. For WT-CFTR expressed in oocytes, these authors presented results somewhat different from ours, showing that NPPB blocked currents with K_D (at −90 mV) of 166 μM and voltage-dependence of 0.24. In contrast, our results suggest that the affinity for NPPB is somewhat higher, and that the voltage-dependence for NPPB and DPC are nearly identical. This points to the importance of studying the two drugs in the same system under identical conditions. Two mutants were studied by Walsh: K335E, predicted to be at the extracellular end of TM6, and R347E, predicted to be at the cytoplasmic end of TM6. Blockade of K335E-CFTR was diminished (K_D = 371 μM) while the voltage-dependence was not affected. This is similar to our results with K335F-CFTR [35]. Block of R347E-CFTR was also reduced (K_D = 1573 μM) and the voltage-dependence was increased significantly. The effect of the K335E mutation is probably representative of a through-space interaction, wherein the negative charge introduced impedes the approach of the negatively charged drug, rather than disruption of an intimate interaction between NPPB and this lysine. It would be interesting to know how block by NPPB was affected by loss of function mutations (such as alanine substitutions), in contrast to gain of function mutations (such as this glutamic acid substitution). In this regard, our whole-cell data suggested that S341 provides an important component to the binding site for NPPB and for DPC, as mutation S341A reduced the efficacy of both drugs. The results of the R347E mutation studied by Walsh [56] are difficult to interpret because this mutation causes disruption of channel structure due to loss of a salt bridge with an aspartic acid in TM8 [5]. Hence, we believe that the binding pocket for arylaminobenzoates lies in a region between S341 in TM6 and T1134 in TM12, although other amino acids may also contribute, particularly for the larger congeners such as NPPB.

Basis of pH-Dependence

While unblocked macroscopic CFTR currents are not apparently sensitive to small deviations around normal bath pH, the apparent efficacy with which both NPPB and DPC block whole-cell CFTR currents is sensitive to bath pH. Incubation with the drug at reduced bath pH increased the magnitude of block at all concentrations tested. Incubation at increased bath pH reduced the magnitude of block. These results may be due to both direct effects on drug-protein interactions and indirect effects due to differential loading, resulting in changes in the actual cytoplasmic concentration of drug. The arylaminobenzoates are lipophilic molecules, with pK_a values of 3–5 [60]. Experimentally determined values are ~4.5 for NPPB [58] and 4.2 for DPC [51]. Using an average pK_a value of 4.3 and calculating the fraction of charged molecules *(C)* at each pH according to [58]

$$C = K_a/(K_a + [H^+]_o) \quad (4)$$

>99% of the drug molecules are charged at both pH 6.5 and 7.5. However, incubation under conditions of reduced bath pH increases by tenfold the small fraction of drug molecules that are uncharged, due to protonation of the carboxylate moiety. Decreased bath pH (from 7.5 to 6.5) results in more drug entering the oocyte through the membrane lipid during incubation, providing more ionized drug inside the cell. This results in a reduction in the apparent dissociation constant at each voltage (Table

1). DPC and NPPB are approximately equally sensitive to this effect. Similar effects of bath pH on NPPB block of cardiac CFTR have been described [58]. When NPPB was injected into the oocyte cytoplasm, the extent of blockade was insensitive to changes in bath pH [58]. However, changes in voltage-dependence were not tested in this study.

In our experiments, three observations suggest that acidic conditions also affect blockade in other, more direct ways. First, the nonstationary analysis allowed us to rapidly test the effects of changes in bath pH. Comparison of the efficacy of DPC at pH 7.5 when the drug was loaded under this condition or following loading at pH 6.5 and acute exposure to pH 7.5 shows that shifting the pH between 6.5 and 7.5 affects the affinity in a manner unrelated to drug loading. If the difference in efficacy at pH 7.5 using these two protocols (gray bars in Fig. 8) were due to changes in the concentration of ionized drug, we would expect that the degree of block when loaded at pH 6.5 would be greater than the degree of block when loaded at pH 7.5. Instead, the opposite is found. In other words, the difference between the black and gray bars in Protocol #1 of Fig. 8 are due to effects on both drug loading and drug-protein interactions. If we assume that the cytoplasmic concentration of charged DPC did not change extensively in one minute, then the difference between black and gray bars in Protocol #2 of Fig. 8 is strictly due to effects of pH on drug-protein interaction.

A second observation is that decreasing bath pH does not have the same fold-effect on the apparent K_D for WT- and T1134F-CFTR (Table 1). We can make use of the combined data from whole-cell experiments in this study to estimate the effective cytoplasmic DPC concentration, because we know the K_D calculated from DPC block of single channels ($K_D^{s\text{-}c}$) [33, 35], as follows:

$$[DPC]_{cyto} = K_D^{s\text{-}c}/(I/(I_o\text{-}I)) \quad (5)$$

Using Eq. (5) and I/I_o data from a number of bath DPC concentrations for WT (10 μM to 1 mM) and one concentration for T1134F-CFTR (100 μM) allows us to estimate the effective $[DPC]_{cyto}$ as a function of $[DPC]_{bath}$, which exhibits a linear relationship at pH 7.5 with $r^2 = 0.98$. With 100 μM drug in the bath and assuming that loading is allowed to run to completion, we calculate that the drug concentration in the cell reaches very similar values for WT- and T1134F-CFTR (84.3 ± 4.3 μM for WT and 74.5 ± 4.9 μM for T1134F-CFTR (mean ± SD; $P > 0.17$)). If the effects of reduced bath pH only reflected alteration of the extent of drug loading, we would expect that this effect would impact equally the currents measured from oocytes expressing WT-CFTR and T1134F-CFTR. However, the calculated effective $[DPC]_{cyto}$ at pH 6.5 was significantly different between the two variants: 143.3 ± 7.4 μM and 216.8 ± 12.1 μM for WT and T1134F-CFTR, respectively (mean ± SD; $P < 0.002$). It is unlikely that drug loading differed in oocytes expressing these two forms of CFTR, and active transport of DPC into the cell has not been shown. The increased effective $[DPC]_{cyto}$ at pH 6.5 reflects an effect of low pH on the drug-protein interaction, resulting in enhanced affinity. It would be interesting to know how bath pH affects the kinetics of blockade studied in single-channels.

Finally, the voltage dependence of block by both DPC and NPPB is sensitive to pH. This result is not due to the effects of pH on drug loading, because voltage dependence is not affected by drug concentration [33]. In the WT channel and T1134F-CFTR, the voltage dependence of block by DPC was reduced at pH 6.5. In S341A-CFTR, the voltage dependence of block was increased at pH 6.5. This is consistent with the notion that S341 serves as a primary determinant of the binding energy for DPC. In contrast to these results with DPC, the voltage dependence of block by NPPB was reduced by low pH in the WT channel and in both the S341A-CFTR and T1134F-CFTR channels. Hence, it seems probable that titratable residues may contribute to the binding site for DPC and NPPB in the WT channel.

It is possible that changing bath pH alters the electrostatic environment within the pore, leading to a change in the voltage profile. This would likely lead to alteration of the voltage dependence of blockade by the charged drugs. Where might these effects of pH take place? Histidine is the only amino acid with a pK in the appropriate range to be greatly affected by these small changes in bath pH. Several histidines are found in the major cytoplasmic domains that control activation of CFTR. However, the lack of overt pH-dependence of unblocked currents suggests that differential protonation of these residues in this pH range is not important to channel function. One TM domain, TM3, has a histidine located near the predicted cytoplasmic end of this alpha helix. On the basis of cysteine-scanning, TM3 has been proposed to line the pore [1]; perhaps this is the residue whose protonation state regulates block by DPC and NPPB. Equally likely are the several histidines that are found in the cytoplasmic loops (CL) linking TM domains, particularly CL1, CL3, and CL4. Structural changes in these loops alter the stability of the open state of CFTR [42, 43, 65]. Hence, it may be that pH-induced changes in the interaction of the major cytoplasmic domains with the histidine-containing cytoplasmic loops regulates the structure of the pore such that affinity and voltage dependence of block by DPC and NPPB are altered. If true, this would provide further evidence that gating and permeation are linked events in CFTR [69]. Of the extracellular loops of CFTR, only one (ECL4) includes a histidine residue. However, as this is predicted to lie outside of the membrane field, it is unclear how differential protonation of this residue could alter

blockade by drugs that enter the pore from the cytoplasmic side. Mutagenesis of these residues could be used to address this issue.

Conclusions

The present study clarifies our understanding of the mechanism of block of the CFTR Cl^- channel by arylaminobenzoates as simple pore-blockade. It also provides initial data toward identification of the binding region for NPPB. DPC and NPPB sense overlapping yet different regions of the pore. Although these drugs are relatively similar in their block of the WT channel, in mutants where the pore structure has changed, that change impacts block by NPPB and DPC in different ways. The blocking behavior of both of these drugs is sensitive to bath pH, implicating titratable residues in their binding regions.

We thank Drs. John Pooler and David Dawson for reviewing an early version of the manuscript. This research was supported by the Cystic Fibrosis Foundation (MCCART96P0) and the American Heart Association (9820032SE).

References

1. Akabas, M.A. 1998. Channel-lining residues in the M3 membrane-spanning segment of the cystic fibrosis transmembrane conductance regulator. *Biochemistry* **37:**12233–12240
2. Burckhardt, B.-C., Kroll, B., Frömter, E. 1992. Proton transport mechanism in the cell membrane of *Xenopus laevis* oocytes. *Pfluegers. Arch.* **420:**78–82
3. Cabantchik, Z.I., Greger, R. 1992. Chemical probes for anion transporters of mammalian cell membranes. *Am. J. Physiol.* **262:**C803–C827
4. Colquhoun, D., Hawkes, A.G. 1995. The principles of the stochastic interpretations of ion-channel mechanisms. *In:* Single-Channel Recording. B. Sakmann and E. Neher, editors. pp. 397–482. Plenum Press, New York
5. Cotten, J.F., Welsh, M.J. 1999. Cystic fibrosis-associated mutations at arginine 357 alter the pore architecture for CFTR: Evidence for disruption of a salt bridge. *J. Biol. Chem.* **274:**5429–5435
6. Cousin, J.L., Motais, R. 1979. Inhibition of anion permeability by amphiphilic compounds in human red cell: evidence for an interaction of niflumic acid with the band 3 protein. *J. Membrane Biol.* **46:**125–153
7. Cunningham, S.A., Worrell, R.T., Benos, D.J., Frizzell, R.A. 1992. cAMP-stimulated ion currents in *Xenopus* oocytes expressing CFTR cRNA. *Am. J. Physiol.* **262:**C783–C788
8. Dawson, D.C., Smith, S.S., Mansoura, M.K. 1999. CFTR: Mechanism of anion conduction. *Physiol. Rev.* **79:**S47–S45
9. DiStefano, A., Wittner, M., Schlatter, E., Lang, H.J., Englert, H., Greger, R. 1985. Diphenylamine-2-carboxylate, a blocker of the Cl^--conductive pathway in Cl^--transporting epithelia. *Pfluegers. Arch.* **405**(Suppl. 1):S95–S100
10. Doughty, J.M., Miller, A.L., Langton, P.D. 1998. Nonspecificity of chloride channel blockers in rat cerebral arteries: block of the L-type calcium channel. *J. Physiol.* **507:**433–439
11. Doyle, D.A., Cabral, J.M., Pfuetzner, R.A., Kuo, A., Gulbis, J.M., Cohen, S.L., Hait, B.T., MacKinnon, R. 1998. The structure of the potassium channel: molecular basis of K^+ conduction and selectivity. *Science* **280:**69–77
12. Drumm, M.L., Wilkinson, D.J., Smit, L.S., Worrell, R.T., Strong, T.V., Frizzell, R.A., Dawson, D.C., Collins, F.S. 1992. Chloride conductance expressed by ΔF508 and other mutant CFTRs in *Xenopus* oocytes. *Science* **254:**1797–1799
13. Fenwick, E.M., Marty, A., Neher, E. 1982. Sodium and calcium channels in bovine chromaffin cells. *J. Physiol.* **331:**599–635
14. Flower, R.J. 1974. Drugs which inhibit prostaglandin biosynthesis. *Pharmacol. Rev.* **26:**33–67
15. Gadsby, D.C., Nairn, A.C. 1997. Regulation of CFTR channel gating. *Trends Biochem. Sci.* **19:**512–518
16. Gögelein, H., Dahlem, D., Englert, H.C., Lang, H.J. 1990. Flufenamic acid, mefenamic acid and niflumic acid inhibit single nonselective cation channels in the rat exocrine pancreas. *FEBS Lett.* **268:**79–82
17. Greger, R. 1990. Chloride channel blockers. *Methods Enzymol.* **191:**793–810
18. Hanrahan, J.W., Tabcharani, J.A. 1990. Inhibition of an outwardly rectifying anion channel by HEPES and related buffers. *J. Membrane Biol* **116:**65–77
19. Heisler, S. 1991. Antagonists of epithelial chloride channels inhibit cAMP synthesis. *Can. J. Physiol. Pharmacol.* **69:**501–506
20. Hille, B. 1992. Ionic Channels of Excitable Membranes. Sinauer Associates, pp. 607 Sunderland, Massachusetts
21. Hosoya, Y., Yamada, M., Ito, H., Kurachi, Y. 1996. A functional model for G protein activation of the muscarinic K^+ channel in guinea pig atrial myocytes. *J. Gen. Physiol.* **18:**485–495
22. Ishihara, H., Welsh, M.J. 1997. Block by MOPS reveals a conformational change in the CFTR pore produced by ATP hydrolysis. *Am. J. Physiol.* **273:**C1278–C1289
23. Kunzelmann, K., Tilmann, M., Hansen, Ch.P., Greger, R. 1991. Inhibition of epithelial chloride channels by cytosol. *Pfluegers. Arch.* **418:**479–490
24. Lerma, J., Martín del Río, R. 1992. Chloride transport blockers prevent N-methyl-D-aspartate receptor-channel complex activation. *Mol. Pharmacol.* **41:**217–222
25. Lester, H.A. 1991. Strategies for studying permeation at voltage-gated ion channels. *Annu. Rev. Physiol.* **53:**477–496
26. Linsdell, P., Hanrahan, J.W. 1996. Disulphonic stilbene block of cystic fibrosis transmembrane conductance regulator Cl^- channels expressed in a mammalian cell line, and its regulation by a critical pore residue *J. Physiol.* **496:**687–693
27. Linsdell, P., Tabcharani, J.A., Hanrahan, J.W. 1997. Multi-ion mechanism for ion permeation and block in the cystic fibrosis transmembrane conductance regulator chloride channel. *J. Gen. Physiol.* **110:**365–377
28. Linsdell, P., Tabcharani, J.A., Rommens, J.M., Hou, Y.-X., Chang, X.-B., Tsui, L.-C., Riordan, J.R., Hanrahan, J.W. 1997. Permeability of wild-type and mutant cystic fibrosis transmembrane conductance regulator chloride channels to polyatomic anions. *J. Gen. Physiol.* **110:**355–364
29. Linsdell, P., Zheng, S.-X., Hanrahan, J.W. 1998. Non-pore lining amino acid side chains influence anion selectivity of the human CFTR Cl^- channel expressed in mammalian cell lines. *J. Physiol.* **512:**1–16
30. Ma, J., Zhao, J., Drumm, M.L., Xie, J., Davis, P.B. 1997. Function of the R domain in the cystic fibrosis transmembrane conductance regulator chloride channel. *J. Biol. Chem.* **272:**28133–28141
31. MacKinnon, R., Miller, C. 1989. Mutant potassium channels with altered binding of charybdotoxin, a pore-blocking peptide inhibitor. *Science* **245:**1382–1385
32. Mansoura, M.K., Smith, S.S., Choi, A.D., Richards, N.W., Strong,

T.V., Drumm, M.L., Collins, F.S., Dawson, D.C. 1998. Cystic fibrosis transmembrane conductance regulator (CFTR) anion binding as a probe of the pore. *Biophys. J.* **74:**1320–1332

33. McCarty, N.A., McDonough, S., Cohen, B.N., Riordan, J.R., Davidson, N., Lester, H.A. 1993. Voltage-dependent block of the cystic fibrosis transmembrane conductance regulator Cl^- channel by two closely related arylaminobenzoates. *J. Gen. Physiol.* **102:**1–23
34. McCarty, N.A., Zhang, Z.-R. 1998. Residues near the extracellular end of TM6 and TM12 in CFTR contribute to anion selectivity. *Biophys. J.* **74:**A395 (*Abst.*)
35. McDonough, S., Davidson, N., Lester, H.A., McCarty, N.A. 1994. Novel pore-lining residues in CFTR that govern permeation and open-channel block. *Neuron* **13:**623–634
36. Poronnik, P., Ward, M.C., Cook, D.I. 1992. Intracellular Ca^{2+} release by flufenamic acid and other blockers of the non-selective cation channel. *FEBS Lett.* **296:**245–248
37. Quick, M.W., Naeve, J., Davidson, N., Lester, H.A. 1992. Incubation with horse serum increases viability and decreases background neurotransmitter uptake in *Xenopus* oocytes. *BioTechniques* **13:**358–362
38. Rich, D.P., Anderson, M.P., Gregory, R.J., Cheng, S.H., Paul, S., Jefferson, D.M., McCann, J.D., Klinger, K.W., Smith, A.E., Welsh, M.J. 1990. Expression of cystic fibrosis transmembrane conductance regulator corrects defective chloride channel regulation in cystic fibrosis airway epithelial cells. *Nature* **347:**358–363
39. Riordan, J.R., Rommens, J.M., Kerem, B.-S., Alon, N., Rozmahel, R., Grzelczak, Z., Zielenski, J., Lok, S., Plavsic, N., Chou, J.-L., Drumm, M.L., Iannuzzi, M.C., Collins, F.S., Tsui, L.-C. 1989. Identification of the cystic fibrosis gene: cloning and characterization of complementary DNA. *Science* **245:**1066–1072
40. Schultz, B.D., DeRoos, A.D.G., Venglarik, C.J., Singh, A.K., Frizzell, R.A., Bridges, R.J. 1996. Glibenclamide blockade of CFTR chloride channels. *Am. J. Physiol.* **271:**L192–L200
41. Schultz, B.D., Singh, A.K., Devor, D.C., Bridges, R.J. 1999. Pharmacology of CFTR chloride channel activity. *Physiol. Rev.* **79:**S109–S144
42. Seibert, F.S., Linsdell, P., Loo, T.P., Hanrahan, J.W., Clarke, D.M., Riordan, J.R. 1996. Disease-associated mutations in the fourth cytoplasmic loop of cystic fibrosis transmembrane conductance regulator compromise biosynthetic processing and chloride channel activity. *J. Biol. Chem.* **271:**15139–15145
43. Seibert, F.S., Linsdell, P., Loo, T.W., Hanrahan, J.W., Riordan, J.R., Clarke, D.M. 1996. Cytoplasmic loop three of cystic fibrosis transmembrane conductance regulator contributes to regulation of chloride channel activity. *J. Biol. Chem.* **271:**27493–27499
44. Sheppard, D.N., Robinson, K.A. 1997. Mechanism of glibenclamide inhibition of cystic fibrosis transmembrane conductance regulator Cl^- channels expressed in a murine cell line. *J. Physiol.* **503:**333–345
45. Sheppard, D.N., Welsh, M.J. 1992. Effect of ATP-sensitive K^+ channel regulators on cystic fibrosis transmembrane conductance regulator chloride currents. *J. Gen. Physiol.* **100:**573–592
46. Sheppard, D.N., Welsh, M.J. 1999. Structure and function of the CFTR chloride channel. *Physiol. Rev.* **79:**S23–S45
47. Smit, L.S., Wilkinson, D.J., Mansoura, M.K., Collins, F.S., Dawson, D.C. 1993. Functional roles of the nucleotide-binding folds in the activation of the cystic fibrosis transmembrane conductance regulator. *Proc. Natl. Acad. Sci. USA* **90:**9963–9967
48. Smith, S.S., Mansoura, M.K., Schafer, J.A., Cooke, C.R., Shariat-Madar, Z., Sun, F., Dawson, D.C. 1997. The fifth putative transmembrane helix of CFTR contributes to the pore architecture. *Biophys. J.* **72:**A365(*Abstr.*)
49. Stutts, M.J., Henke, D.C., Boucher, R.C. 1990. Diphenylamine-2-carboxylate (DPC) inhibits both Cl^- conductance and cyclooxygenase of canine tracheal epithelium. *Pfluegers. Arch.* **415:**611–616
50. Tabcharani, J.A., Linsdell, P., Hanrahan, J.W. 1997. Halide permeation in wild-type and mutant cystic fibrosis transmembrane conductance regulator chloride channels. *J. Gen. Physiol.* **110:**341–351
51. Terada, H., Muraoka, S., Fujita, T. 1974. Structure-activity relationships of fenamic acids. *J. Med. Chem.* **17:**330–334
52. Tilmann, M., Kunzelmann, K., Fröbe, U., Cabantchik, I., Lang, H.J., Englert, H.C., Greger, R. 1991. Different types of blockers of the intermediate-conductance outwardly rectifying chloride channel in epithelia. *Pfluegers. Arch.* **418:**556–563
53. Tominaga, M., Horie, M., Okada, Y. 1994. Additional similarity of cardiac cAMP-activated Cl^- channels to CFTR Cl^- channels. *Jap. J. Physiol.* **44(2):**S215–S218
54. Vandorpe, D., Kizer, N., Ciampollilo, F., Moyer, B., Karlson, K., Guggino, W.B., Stanton, B.A. 1995. CFTR mediates electrogenic chloride secretion in mouse inner medullary collecting duct (mIMCD-K2) cells. *Am. J. Physiol.* **269:**C683–C689
55. Venglarik, C.J., Schultz, B.D., DeRoos, A.D.G., Singh, A.K., Bridges, R.J. 1996. Tolbutamide causes open channel blockade of cystic fibrosis transmembrane conductance regulator Cl^- channels. *Biophys. J.* **70:**2696–2703
56. Walsh, K.B., Long, K.J., Shen, X. 1999. Structural and ionic determinants of 5-nitro-2-(3-phenylpropylamino)-benzoic acid block of the CFTR chloride channel. *Br. J. Pharmacol.* **127:**369–376
57. Walsh, K.B., Wang, C. 1996. Effect of chloride channel blockers on the cardiac CFTR chloride and L-type calcium currents. *Cardiovasc. Res.* **32:**391–399
58. Walsh, K.B., Wang, C. 1998. Arylaminobenzoate block of the cardiac cyclic AMP-dependent chloride current. *Mol. Pharmacol.* **53:**539–546
59. Wang, F., Zeltwanger, S., Yang, I.C., Nairn, A.C., Hwang, T.-C. 1998. Actions of genistein on cystic fibrosis transmembrane conductance regulator channel gating: Evidence for two binding sites with opposite effects. *J. Gen. Physiol.* **111:**477–490
60. Wangemann, P., Wittner, M., DiStefano, A., Englert, H.C., Lang, H.J., Schlatter, E., Greger, R. 1986. Cl^- channel blockers in the thick ascending limb of the loop of Henle. Structure activity relationship. *Pfluegers. Arch.* **407:**S128–S141
61. White, M.M., Aylwin, M. 1990. Niflumic and flufenamic acids are potent reversible blockers of Ca^{2+}-activated Cl^- channels in *Xenopus* oocytes. *Mol. Pharmacol.* **37:**720–724
62. Wilkinson, D.J., Mansoura, M.K., Watson, P.Y., Smit, L.S., Collins, F.S., Dawson, D.C. 1996. CFTR: the nucleotide binding folds regulate the accessibility and stability of the activated state. *J. Gen. Physiol.* **107:**103–119
63. Woodhull, A.M. 1973. Ionic blockage of sodium channels in nerve. *J. Gen. Physiol.* **61:**687–708
64. Wu, G., Hamill, O.P. 1992. NPPB block of Ca^{++}-activated Cl^- currents in *Xenopus* oocytes. *Pfluegers. Arch.* **420:**227–229
65. Xie, J., Drumm, M.L., Zhao, J., Ma, J., Davis, P.B. 1996. Human epithelial cystic fibrosis transmembrane conductance regulator without exon 5 maintains partial chloride channel function in intracellular membranes. *Biophys. J.* **71:**3148–3156
66. Yellen, G., Jurman, M.E., Abramson, T., MacKinnon, R. 1991. Mutations affecting internal TEA blockade identify the probable pore-forming region of a K^+ channel. *Science* **251:**939–942
67. Zeltwanger, S., Wang, F., Wang, G.-T., Gillis, K.D., Hwang, T.-C. 1999. Gating of cystic fibrosis transmembrane conductance regulator chloride channels by adenosine triphosphate hydrolysis: Quantitative analysis of a cyclic gating scheme. *J. Gen. Physiol.* **113:**541–554
68. Zhang, Z.-R., McCarty, N.A. 1998. A comparison of probes for structure/function experiments in CFTR. *Ped. Pulmonol.* **17:**224–225 (*Abstr.*)
69. Zhang, Z.-R., McDonough, S.I., McCarty, N.A. 2000. Interaction between permeation and gating in a putative pore-domain mutant in CFTR. *Biophys. J.* (*in press*)